sterically induced nonplanarity of TMOX. Unfortunately, the only information available on this point relates to NMR studies, and inferences based thereon by Siddall and Good.[14] In any event, such a nonplanarity would lead to an expected decrease in the $\pi_\ominus/\pi_\oplus$ separation, the n_+/n_- separation remaining relatively unaffected. Consequently, it is possible that the near degeneracy of the n_+, $\pi_\oplus$, and $\pi_\ominus$ ionization events exhibited in Figure 5c is attributable, in part, to bending and not *solely* to *N*-methylation effects as implied above. In addition, the diffuseness of the 9 eV PES band may be due not so much to near degeneracy of these three events (i.e., the n_+, $\pi_\oplus$, and $\pi_\ominus$ ionizations) as to the existence of a statistical ensemble of variously twisted TMOX species in the gas phase.

Correlation Diagrams. The results of CNDO/s computations are summarized in Figure 3 and may be compared with the experimental correlation diagram of Figure 4. This comparison is massively impressive, particularly in the lower ionization energy regime. Any assignments which might be made in the higher ionization energy regime (apart from direct comparison with the computational results, a procedure which is more than suspect) would have little foundation; hence, this region is left largely unassigned.

Acknowledgment. This work was supported by contract between the United States Atomic Energy Commission-Biomedical and Environmental Research Physics Program and The Louisiana State University.

References and Notes

(1) J. L. Meeks, H. J. Maria, P. Brint, and S. P. McGlynn, *Chem. Rev.*, in press.
(2) J. L. Meeks, J. F. Arnett, D. B. Larson, and S. P. McGlynn, *Chem. Phys. Lett.*, **30**, 190 (1975).
(3) H. Basch, M. B. Robin, and N. A. Kuebler, *J. Chem. Phys.*, **49**, 5007 (1968).
(4) D. B. Larson and S. P. McGlynn, *J. Mol. Spectrosc.*, **47**, 469 (1973).
(5) C. R. Brundle, D. W. Turner, M. B. Robin, and H. Basch, *Chem. Phys. Lett.*, **3**, 292 (1969).
(6) J. L. Meeks, J. F. Arnett, D. B. Larson, and S. P. McGlynn, *J. Am. Chem. Soc.*, **97**, 3905 (1975).
(7) D. B. Larson, J. F. Arnett, and S. P. McGlynn, *J. Am. Chem. Soc.*, **95**, 6928 (1973).
(8) The program used was QCPE:CNDO 174.
(9) Geometrical parameters used in CNDO/s were: bond lengths and bond angles for PBA were those of D. R. Davis and J. J. Blum, *Acta Crystallogr.*, **8**, 129 (1955). Standard structural parameters were used for the CH_3 groups of PBA derivatives. Urea: A. Caron and J. Donahue, *ibid.*, **17**, 544 (1964). *cis*-Glyoxal: E. M. Ayerst and J. R. C. Duke, *ibid.*, **7**, 588 (1954).
(10) J. R. Swenson and R. Hoffmann, *Helv. Chim. Acta*, **53**, 2331 (1970).
(11) T. Koopmans, *Physica* (Utrecht), **1**, 104 (1934).
(12) D. O. Cowan, R. Gleiter, J. A. Hashmall, E. Heilbronner, and V. Hornung, *Angew. Chem., Int. Ed. Engl.*, **10**, 401 (1971).
(13) D. W. Turner, C. Baker, A. D. Baker, and C. R. Brundle, "Molecular Photoelectron Spectroscopy", Wiley-Interscience, New York, N.Y., 1970.
(14) T. H. Siddall and M. L. Good, *J. Inorg. Nucl. Chem.*, **29**, 149 (1967); M. L. Good, T. H. Siddall, and R. N. Wilhite, *Spectrochim. Acta, Part A*, **23**, 1161 (1967).

Nicotinamide Adenine Dinucleotide (NAD^+) and Related Compounds. Electrochemical Redox Pattern and Allied Chemical Behavior

Conrad O. Schmakel, K. S. V. Santhanam, and Philip J. Elving*[1]

Contribution from The University of Michigan, Ann Arbor, Michigan 48104.
Received November 26, 1974

Abstract: Important aspects of the electrochemical redox pattern and related chemical behavior of nicotinamide adenine dinucleotide (NAD^+) have been examined on the basis of electrochemical, spectrophotometric, chemical, and enzymatic studies of the coenzyme, $NADP^+$, deamino-NAD^+, their reduction products, and related nicotinamides and adenines. The artifacts introduced into the observed electrochemical patterns by coenzyme and reduction product adsorption at the solution-electrode interface can be removed by addition of a more strongly adsorbed species. An initial reversible one-electron (1e) addition to the pyridinium ring produces a free radical, which dimerizes (rate constants at pH 9 and 30° are $2.4 \times 10^6\ M^{-1}$ sec^{-1} for NAD^+, 1.6×10^6 for $NADP^+$ and 1.7×10^6 for deamino-NAD^+; activation energies and frequency factors were determined). At more negative potential, the radical is reduced (1e, 1 H^+) to a dihydropyridine, largely 1,4-NADH; some 1,6-NADH is also formed, indicating the lesser specificity of electrochemical reduction as compared with enzymatic. At sufficiently positive potential, dimer and dihydropyridine are oxidized to NAD^+; the dimer is much more easily oxidized. The dimer is not directly reduced electrochemically within the available potential range. Both reduction products hydrolyze; rate increases with decreasing pH; at a given pH, dimer is less stable than dihydropyridine.

The pyridine nucleotide, nicotinamide adenine dinucleotide (NAD^+; diphosphopyridine nucleotide, DPN^+; coenzyme I) (Figure 1), is a coenzyme for the dehydrogenase enzymes which catalyze redox processes in virtually all biological systems, involving transfer of hydrogen between substrate and coenzyme, e.g., alcohol dehydrogenase (ADH) catalyzes oxidation of ethanol to acetaldehyde and simultaneous reduction of NAD^+ to $NADH^2$ via effective net transfer of a hydride ion from alcohol to C(4) of the pyridine ring.[3]

The gross reversibility of the NAD^+/NADH redox couple under physiological conditions has prompted extensive study by polarographic techniques.[4] While the basic reduction pathway of NAD^+ has been well established (cf. Redox Path), certain aspects of its electrochemical and related chemical behavior have been only partially explained or have not been considered. The present investigation was designed to establish more clearly the influence of adsorption of reactant and products at the interface, the postulated electroactivity of the dimer produced on the initial one-electron (1e) reduction, the structure of the product(s) produced on 2e reduction, the magnitudes of rate-controlled

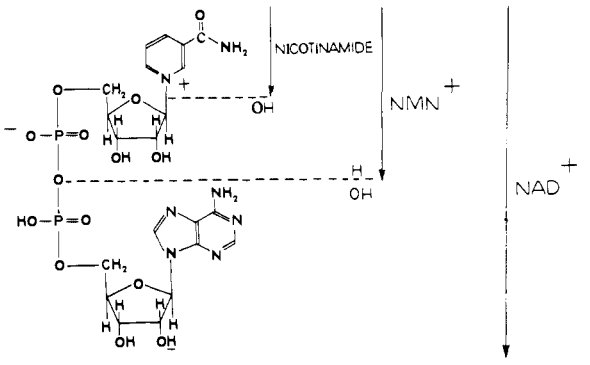

Figure 1. Formula for enzymatically active NAD^+, i.e., β-nicotinamide adenine dinucleotide. The isomer having an α-glycosidic nicotinamide ribose linkage does not exhibit enzymatic activity with yeast ADH. A related coenzyme, nicotinamide adenine dinucleotide phosphate ($NADP^+$), is formed when the underlined H is replaced by a $PO(OH)_2$ group. In deamino-NAD^+ ($DNAD^+$), the adenine moiety is replaced by hypoxanthine.

Table I. Buffer and Background Electrolyte Solutions[a]

Buffer No.	pH range	Composition
1	0.0–1.8	HCl + KCl
2	2.0–8.0	$Na_2HPO_4 \cdot 7H_2O$ + citric acid monohydrate + KCl
3	3.9–5.9	HOAc + NaOAc
3a	5.4	HOAc + NaOAc + Et_4NCl[c]
3b	7.8	H_3BO_3 + KCl + NaOH
4	9.0–10.0	K_2CO_3 + $KHCO_3$
5	9.0–10.0	K_2CO_3 + $KHCO_3$ + KCl[b]
6	9.0–10.0	K_2CO_3 + $KHCO_3$ + Et_4NCl[c]
7	9.0–10.0	NH_3 + NH_4Cl
8	11.0–12.0	KOH + KCl

[a] The final ionic strength of buffer solutions in all experiments was 0.5 *M* unless otherwise stated. [b] KCl concentration: 0.4 *M*. [c] Et_4NCl concentration: 0.4 *M*.

processes, e.g., free radical dimerization, and hydrolytic and oxidative product stability. In particular, perturbation techniques (ac polarography and cyclic voltammetry) were used to study adsorption and kinetics, and product solutions were thoroughly examined.

In addition to the normal β form of NAD^+, α-NAD^+, nicotinamide adenine dinucleotide phosphate ($NADP^+$; triphosphopyridine nucleotide, TPN^+; coenzyme II), deamino-NAD^+ (nicotinamide hypoxanthine dinucleotide; $DNAD^+$), deamino-$NADP^+$ (nicotinamide hypoxanthine dinucleotide phosphate; $DNADP^+$), and the various reduction products derived from these compounds in aqueous media were examined.

Experimental Section

Chemicals, apparatus, and procedures have been described.[5-7] Potentials were measured with respect to the aqueous saturated calomel electrode (SCE). The buffer solutions used, prepared from reagent grade chemicals, are listed in Table I.

The reported analytical data and spectrophotometric assay indicated sufficient purity for polarographic study of the compounds used: adenine, adenosine, adenosine 5′-monophosphate (AMP), sodium adenosine 5′-diphosphate (ADP), dipotassium adenosine 5′-triphosphate (ATP), β-NAD^+, and yeast ADH from Calbiochem; NADH, nicotinamide mononucleotide (NMN^+), reduced nicotinamide mononucleotide (NMNH), α-NAD^+, $NADP^+$, $DNAD^+$, and $DNADP^+$ from Sigma; adenosine diphosphate ribose (ADPR) from Mann Research. Compounds were stored in a desiccator over $CaSO_4$ at 5° or over silica gel.

Solutions containing NAD^+ or its reduction products were assayed enzymatically[8] before and after each controlled potential electrolysis;[7] 6220 was used for the 340-nm molar absorptivity of the reduced coenzyme.[9]

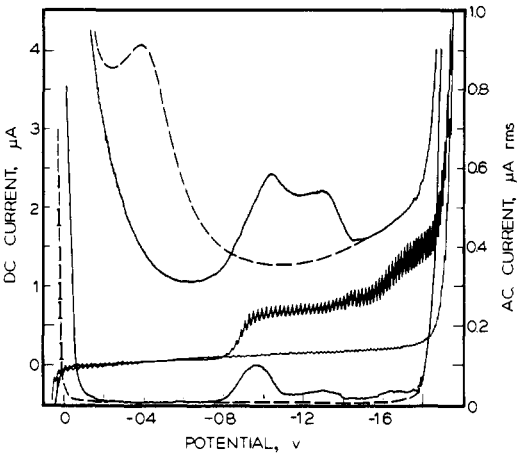

Figure 2. Dc and ac polarograms of NAD^+ (0.31 m*M*) in pH 9.3 KCl/carbonate buffer. Dc polarograms shown with and without electroactive species present. Ac polarograms: solid lines represent in-phase (lower set) and quadrature (upper set) components of total ac current; dashed lines represent corresponding background currents.

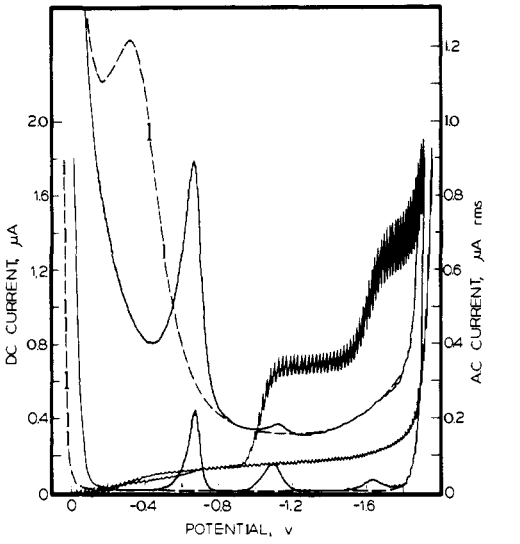

Figure 3. Dc and ac polarograms of NAD^+ (0.31 *M*) in pH 9.6 Et_4NCl/carbonate buffer. Dc polarograms shown with and without electroactive species present. Ac polarograms: solid lines represent in-phase (lower set) and quadrature (upper set) components of total ac current; dashed lines represent corresponding background currents.

Results and Discussion

Although the electrochemical behavior of NAD^+ was surveyed over the pH range of 2–12, catalytic hydrogen evolution[11] at lower pH and NAD^+ decomposition at higher pH resulted in detailed studies being largely confined to pH 9–10, where both reduction waves are simultaneously visible (Figures 2 and 3).

Dc Polarography. Below pH 6, NAD^+ exhibits a single cathodic wave (wave I) (Table II), which, with increasing pH, decreases in height to a limiting value at pH 4–5 and becomes diffusion controlled. Above pH 10, the NAD^+ pattern diminishes because of hydrolysis and a wave due to nicotinamide reduction[5] develops. The decomposition rate increases with pH; after an hour (0.31 m*M* NAD^+; 25°), 1.9% was decomposed at pH 9.5 and 88% at pH 11.8. $E_{1/2}$ is virtually pH independent; the diffusion current constant, I, (1.1–1.3) suggests a 1e faradaic process.

Table II. Variation in Polarographic Behavior of NAD^+ with pH

Buffer No.	pH	Concn, mM	$-E_{1/2}$, V[a]	Wave[b] slope, mV	I[b]	x[c]	Background shift,[d] mV
1	1.0[e]	0.32					270
1	1.0[e]	0.45	(0.90)				
1	1.8[e]	0.45	(0.92)				
2	2.1	0.32	0.89	93	2.35	0.43	230
2	2.9	0.32	0.90	88	1.92	0.38	280
2	4.4	0.31	0.88	67	1.35	0.46	210
3	5.0	0.32	0.88	67	1.20	0.51	250
3	5.0	0.13–2.6	0.91–0.92	58–60	1.1–1.6	0.50	
3	5.4	0.31	0.88	65	1.25		300
2	6.1	0.32	0.89	62	1.22		250
3[b]	7.8	0.74	1.13	59	1.80	0.50	
2	7.1	0.32	0.89	59	1.18	0.50	200
2	8.0	0.32	0.89	59	1.15		120
4	9.0	0.34–1.7	0.91–0.92	60	1.1–1.3		
4	9.3[f]	0.32	0.91		1.22		0
4	9.3[g]	0.32	0.90		1.24		0
5	9.3	0.32	I 0.89		1.19		0
			II 1.62		1.28		
5	9.3[h]	0.32	0.89		1.21		0
4	9.4	0.31	I 0.89	63	1.26	0.49	0
			II 1.67	121	1.70	0.31	
7	9.5[i]	0.32	0.89	65	1.23		0
6	9.6	0.31	I 1.03	70	1.12	0.49	0
			II 1.61	75	1.34	0.52	
8	11.8[j]	0.26	0.90	63			0

[a] Data are for wave I except where Roman numerals are used to indicate the two waves. [b] Wave slope calculated as $(E_{1/4} - E_{3/4})$. Diffusion current constant, $I = i_d/Cm^{2/3}t^{1/6}$. In order to compare relative wave heights, I values have been calculated in some cases for waves whose limiting currents are not diffusion controlled. [c] X is a measure of the dependence of the limiting current (i_l) on the corrected height (h): $\log i_l = X \log h$. Dependence determined by using three to six heights. [d] Shift in background discharge in the presence of the electroactive species compared with that for the supporting electrolyte alone. [e] Wave I not observed. Background discharge begins at a potential where the foot of the NAD^+ wave normally occurs. [f] Ionic strength = 0.03 M. Wave II is ill defined. [g] Ionic strength = 0.10 M. Wave II is ill defined. [h] Ionic strength = 2.0 M. A capacity wave obscures wave II. [i] Data not taken because of the presence of a capacity wave or maximum prior to wave II. [j] Data not taken due to instability of NAD^+ in basic solutions.

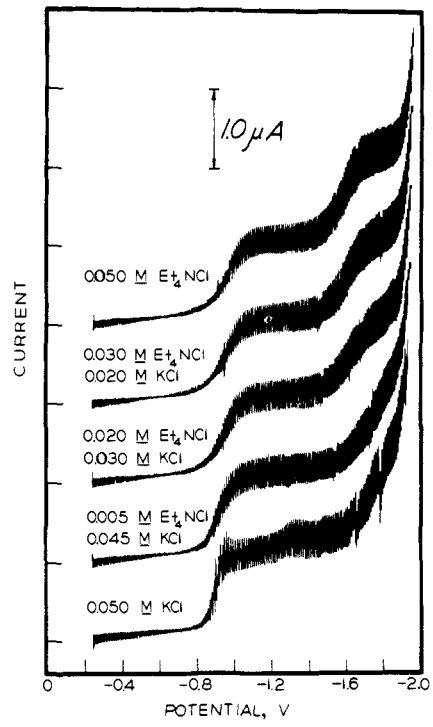

Figure 4. Variation in the dc polarographic behavior of NAD^+ (0.32 mM) with increasing Et_4NCl concentration. All solutions were maintained at 0.10 M ionic strength (0.05 M carbonate buffer plus Et_4NCl and KCl as shown; final pH 9.9).

The positive shift (0.2–0.3 V) of solution discharge on NAD^+ addition, due to catalytic hydrogen evolution, is relatively constant to pH 6 but then decreases; at pH 9, discharge occurs at a potential identical with that for background electrolyte alone.

Wave II is partially obscured by hydrogen evolution below pH 9 and by nicotinamide reduction above pH 10; at pH 6–8, it does not exhibit a limiting portion as does NMN^+ wave II,[6] but gradually merges with solution discharge.

At pH 9–12, a very small anodic wave sometimes seen close to mercury discharge corresponds to formation of a mercury-adenine complex; a similar wave is seen for ADP but not for NMN^+.

1. Behavior at pH 9 to 10. Although NAD^+ wave I shifts relatively little in potential with increasing ionic strength (μ) (Table II), accompanying maxima are affected. At low μ, a slight maximum of the first kind appears on the rising wave and a small maximum of the second kind or capacity wave is seen on the limiting plateau at −1.3 V; wave II appears as an ill-defined shoulder on solution discharge. On addition of 0.0008% Triton or 5 mM Et_4NCl, both maxima disappear and wave I is well defined. With increasing μ, the first maximum disappears, the capacity wave grows in direct proportion and shifts to more negative potential, and wave II appears and grows. Characterization of wave II is difficult because of its proximity to the capacity wave. At 1 M μ, 0.0008% Triton only partially decreases the latter.

The capacity wave is associated with desorption of the dimeric wave I reduction product from the interface. Any factor, which increases the dimer's surface activity, e.g., by lowering its solubility, shifts the wave to more negative potential; shifts of −190, −90, and −50 mV occur, respectively, with increased μ (0.1–2 M), decreased temperature (37.0–1.4°), and increased NAD^+ concentration (0.05–1.93 mM). The wave height is directly proportional to NAD^+ concentration, unaffected by temperature, and, in buffer 5, directly proportional to h. A dc wave would not be expected to accompany desorption which does not produce a faradaic current; however, desorption might cause stirring, which would increase the limiting wave I current.

2. Effect of Et_4N^+. Et_4NCl addition significantly changes the NAD^+ pattern at pH 9–10; e.g., on increasing Et_4NCl concentration at constant μ, wave I shifts negatively and wave II becomes distinct and grows (Figure 4); the solution discharge potential is unchanged. At sufficiently high Et_4NCl concentration (Figures 3 and 4), two well-defined diffusion-controlled waves of about equal height are seen, whose slopes deviate appreciably from that expected for an uncomplicated reversible 1e wave. With increasing NAD^+ concentration (0.013–1.32 mM at pH 9.6), the waves remain of equal height, but $E_{1/2}$ of wave I becomes more positive (−1.09 to −1.00 V) and of wave II more negative (−1.58 to −1.65 V).

A small wave of constant height at −0.6 V (Figure 3) becomes about 0.1 V more negative between 0.13 and 1.20 mM NAD^+; the charging current before this wave is depressed from background level but is identical afterwards.

3. Compounds Related to NAD^+. The behavior of $NADP^+$, $DNAD^+$, $DNADP^+$, and α-NAD^+ (Table III) is generally similar to that of NAD^+. At slightly acidic pH, only wave I is observed; at higher pH (9–10), wave II is also visible. Differences between the five compounds are primar-

Table III. Variation in Polarographic Behavior of $NADP^+$, $DNAD^+$, $DNADP^+$, and α-NAD^+

Buffer No.	pH	Concn, m*M*	$-E_{1/2}$,[a] V	Wave[b] slope, mV	*I*[b]
			$NADP^+$		
2	3.0	0.28	0.91	95	2.0
2	4.4	0.29	0.89	71	1.25
3	5.0	0.28	0.89	74	1.13
3	5.0	0.28	0.95		1.63
		0.61	0.95		0.94
		0.63	0.95	60	1.08
		1.04	0.95	60	1.17
4	9.0	0.39	0.97	60	0.92
		0.52	1.03		0.88
		0.88	1.11		1.10
		1.10	1.11		1.10
4	9.4	0.29	I 0.92	56	1.20
			II 1.69	91	1.54
6	9.6	0.29	I 1.06	79	1.01
			II 1.61	93	1.24
			$DNAD^+$		
2	3.0	0.37	0.93	77	1.31
2	4.4	0.37	0.89	65	1.23
3	5.0	0.37	0.89	64	1.02
3	5.2	0.58	0.93	60	1.31
4	9.3	0.21	0.97	59	
		0.46	0.97		
		0.52	0.97	60	1.24
		0.77	0.96		
		0.94	0.97		1.19
4	9.4	0.37	I 0.91	67	1.13
			II 1.64	94	1.23
6	9.6	0.37	I 1.04	60	0.94
			II 1.60	92	1.07
			$DNADP^+$		
2	3.0	0.26	0.93	94	2.00
2	4.4	0.26	0.91	69	1.29
3	5.0	0.26	0.89	57	1.08
4	9.4	0.26	I 0.93	61	1.15
			II 1.68	93	1.55
			α-NAD^+		
2	3.0	0.46	0.93	77	1.31
2	4.4	0.46	*c*	*c*	*c*
3	5.4	0.46	*c*	*c*	*c*
3a	5.4	0.46	1.07	82	1.14
2	6.1	0.32	0.99	79	1.20
2	7.1	0.32	0.99	86	1.15
5	9.3	0.32	I 0.99	81	1.17
			II 1.58	124	1.26
4	9.4	0.46	I 1.00	74	1.24
			II 1.63	109	1.46
6	9.6	0.46	I 0.97	83	1.11
			II 1.61	88	1.17

[a] Data are for wave I except when Roman numerals are used to indicate the two waves. [b] Headings are explained in Table II. [c] Abnormal wave due to dimer adsorption.

ily due to adsorption (cf. Ac Polarography). On Et_4NCl addition, these compounds as well as NMN^+ [6] exhibit essentially identical behavior (Tables II and III; buffer 6); both waves are well defined.

Ac Polarography.[12] In pH 9.3 buffer 5 (Figure 2),[13] NAD^+ shows a faradaic peak (in-phase component) at −0.97 V (wave I process; quadrature component at −1.04 V) and a barely discernible peak at −1.65 V (wave II process; no detectable quadrature component). Prior to the wave I process, adsorption of NAD^+ depresses the differential double layer (dl) capacity with a minimum at −0.65 V. A quadrature peak at −1.29 V, almost entirely capacitive in nature, is a tensammetric peak resulting from desorption of the wave I product (dimer). Beyond −1.5 V, the dl capacity is the same as for background alone, indicating that the wave II product is not adsorbed over the potential range of its formation.

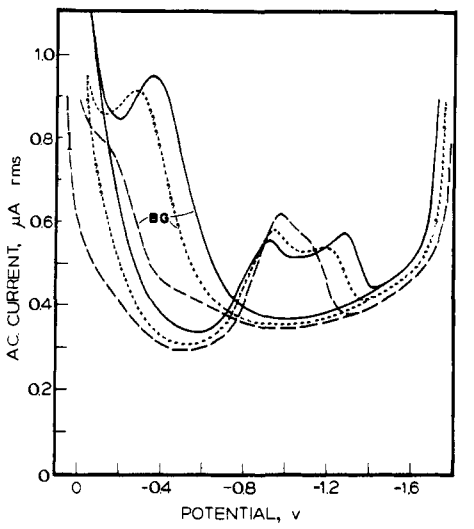

Figure 5. Effect of ionic strength on the adsorption-desorption behavior of the dimeric reduction product of NAD^+. Quadrature components of ac polarograms for NAD^+ (0.32 m*M*) in 0.1 *M* carbonate buffer (pH 9.3) plus KCl where required (dashed line, 0.1 *M* ionic strength; dotted line, 0.5 *M*; solid line, 2.0 *M*; BG indicates background electrolyte base current at the designated ionic strength).

The moderate sensitivity of the ac patterns to experimental variables is confined to adsorption-desorption phenomena; faradaic processes remain about the same. Factors expected to increase dimer surface activity shift the tensammetric peak negatively similar to the corresponding dc capacity wave (Figures 5 and 6). The patterns are virtually unchanged between pH 3 and 12; the dl capacity minimum is constant (−0.64 ± 0.02 V) as is the tensammetric peak (E_s = −1.27 ± 0.03 V), i.e., the NAD^+ adsorption is pH insensitive.

1. Effect of Et_4N^+. Substitution of Et_4NCl for KCl in the background electrolyte, as expected, significantly alters the ac pattern (Figures 2 and 3). In buffer 6, NAD^+ exhibits faradaic peaks at −1.09 and −1.64 V, a peak at zero volt (mercury oxidation), and a tensammetric peak at −0.67 V.

The depressed capacity prior to the latter tensammetric peak indicates that NAD^+ is adsorbed at the interface. In the potential region of the peak, which is more negative than the ecm, NAD^+ is desorbed due to preferential adsorption of Et_4N^+. With increasing NAD^+ concentration (0.13-1.26 m*M*), the peak shifts from −0.64 to −0.73 V and its current increases by a factor of 2.5. With increasing Et_4N^+ concentration, the peak becomes more positive and increases in size. The small dc wave at −0.6 V is due to charging current arising from this desorption-adsorption process. Between the tensammetric and first faradaic peaks, the dl capacity is nearly the same as for background alone, indicating that NAD^+ is not adsorbed. Absence of a change in dl capacity following the two faradaic processes indicates that the reduction products are not adsorbed. Thus, Et_4N^+ is preferentially adsorbed in the potential region following the tensammetric peak. Results are similar for NAD^+ concentration as high as 1.26 m*M*.

2. Behavior of Related Compounds. $NADP^+$, $DNAD^+$, $DNADP^+$, and α-NAD^+ were studied in pH 5.0 acetate and pH 9.4 carbonate buffers. The principal difference between them in the absence of Et_4NCl is in their relative tendencies to adsorb at the interface; each is adsorbed, causing a quadrature component depression prior to wave Ic. The pattern for $NADP^+$ is similar to that of NAD^+.

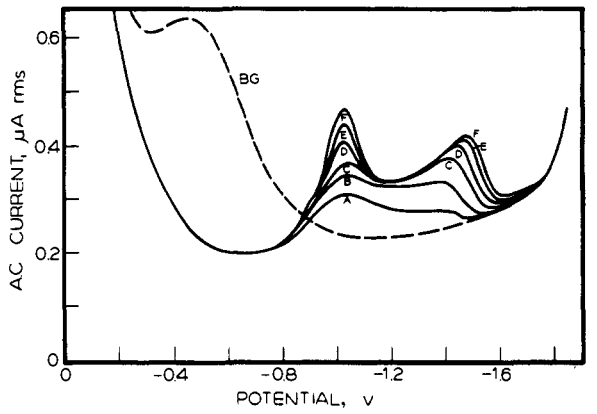

Figure 6. Effect of NAD^+ concentration on the adsorption-desorption behavior of the NAD dimeric reduction product. Quadrature components of ac polarograms for solutions 1.50 M in KCl and 0.25 M in carbonate buffer (pH 9.9) (mM NAD^+ concentration: A, 0.04; B, 0.12; C, 0.34; D, 0.88; E, 1.26; F, 1.76).

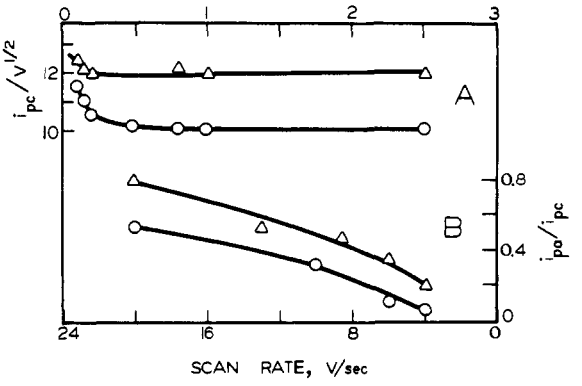

Figure 7. Effect of scan rate (v) on cyclic voltammetry at HMDE of NAD^+ (0.75 mM, circles) and $NADP^+$ (0.85 mM; triangles) at pH 5.0 acetate buffer. A: variation of current function ($i_p/v^{1/2}$) for cathodic peak 1. B: variation of i_{pa}/i_{pc} ratio for peak 1.

$DNAD^+$ is most strongly adsorbed, exhibiting a deep "adsorption well" or depression prior to wave I; its adsorption also causes a depression in the dc charging current.

Similar to NAD^+, each wave I product is adsorbed when formed but is desorbed at more negative potential, e.g., appearance of an ac peak, mainly capacitive in nature, and, in some cases, of a capacity wave on the dc wave I plateau prior to wave II. The most strongly adsorbed dimer is that of α-NAD^+; in acidic solution, its adsorption causes a deep depression in the quadrature current and considerably distorts dc wave I. On Et_4NCl addition, dimer adsorption disappears (Table III).

Ac faradaic peak I currents for all five compounds are considerably less than expected for a reversible 1e process;[14] the magnitude of the difference decreases with increasing frequency (50-1000 Hz). This indicates a chemical reaction following the initial 1e reduction; the reaction cannot be identified as a dimerization, as the necessary diagnostic criteria have not been developed. The second harmonic curve shapes are characteristic of reduction processes influenced by chemical reactions involving the reduced species. The peak heights grow with increasing frequency; at high frequency (500 Hz), an additional derivative pattern is noticeable at −1.32 V.

Cyclic Voltammetry. The behavior of NAD^+ (0.32 mM) was surveyed at pH 0-12 at the hanging mercury drop electrode (HMDE) with a scan rate (v) of 0.1 V/sec, except as otherwise noted.

Below pH 2, a cathodic peak Ic appears as an ill-defined shoulder on solution discharge. With increasing pH, the peak becomes better defined and decreases to a limiting value above pH 6; E_p (−0.93 V) is independent of pH. A prewave at the foot of the peak, whose definition increases with v, is probably due to adsorption of reduction product. At v > 10 V/sec and pH below 7, a small cathodic peak (E_p = −1.35 V) appears, which grows with increasing v and may be due to adenine reduction and/or dimer desorption.

In alkaline solution, peak IIc (E_p = −1.6 V) also appears. The fact that its i_p is less than 10% that of Ic supports nonreduction of the wave I product in the wave II process; i.e., most of the NAD^+ in the vicinity of the electrode forms the 1e product before the potential for formation of the 2e product is reached and the IIc current is due to reduction of NAD^+ which diffuses through the depleted layer.[15]

Potential sweep reversal after appearance of Ic or IIc (v < 7 V/sec) yields anodic peak Ia (−0.2 V) due to dimer oxidation; the 2e reduction product is oxidized at potential more positive than mercury oxidation. In alkaline solution, repetitive cycling in a potential region, which includes Ic and Ia, does not diminish the Ic current, indicating that the oxidation regenerates the original electroactive species. At v > 10 V/sec, Ia is barely seen due to oxidation of the free radical before it can dimerize. Above pH 5, Ia is pH independent (E_p = −0.25 V); below pH 5 (buffers without Et_4N^+), E_p = −0.080 − 0.037pH, and i_p decreases rapidly with decreasing pH due to instability of the dimer.

The peak Ic $i_p/v^{1/2}$ ratio is constant at pH 9.4 (buffer 5) for v of 0.025-0.5 V/sec, but E_p becomes 30 mV more negative; $i_p/v^{1/2}$ for Ia is also constant. A small decrease in the Ic ratio on increasing v to 10 V/sec (Figure 7) is characteristic of reversible charge transfer followed by dimerization; the $E_p - E_{1/2}$ difference at low v is 39-42 mV (pH 5-9) compared with a theoretical $39/n$ mV.[16] At v > 10 V/sec, on the return sweep, Ia decreases and disappears, and a new anodic peak appears whose E_p difference of 60 mV from Ic indicates that it is due to reversible oxidation of the primary 1e reduction product of the Ic process.

$NADP^+$ behaves similarly (Figure 7); the dimer is oxidized at −0.2 V; above v = 10 V/sec, a well-defined anodic peak complementary to the initial 1e reduction is observed ($E_{pa} - E_{pc}$ = 60 mV). $DNAD^+$ shows a single cathodic peak (E_p = −1.16 at pH 5.2 and −1.21 at pH 9.3) with the characteristics expected for dimerization; the dimer is oxidized (pH 9.3) at E_p = −0.06 V.

The behavior of NAD^+ at the pyrolytic graphite electrode (PGE) is essentially the same as at the HMDE, e.g., 1e reduction at −1.05 V to a product, which is oxidized back to NAD^+ at −0.14 V. The 2e product is oxidized at 0.4 V.

Controlled Electrode Potential Electrolysis. 1. Wave I Process. Electrolysis at a potential on the NAD^+ wave Ic plateau (−1.2 or −1.3 V) at pH 5.6-9.6 gave an average faradaic n of 1.01 (14 electrolyses of 0.98-1.26 mM NAD^+; standard deviation = 0.02). Time-log current plots were linear, showing a first-order electrolysis rate and the absence of mechanistic complications. In each case, a transient greenish-yellow color appeared, which reached maximum intensity when electrolysis was 80-90% complete. On continuation of electrolysis for 0.5 hr after current fell to background level, the current was unchanged but the color diminished, yielding a clear faintly yellow solution. Apparently, at least one product is formed, which absorbs in the visible and slowly decomposes to a compound stable at the applied potential.

Both NAD^+ cathodic waves were absent from polaro-

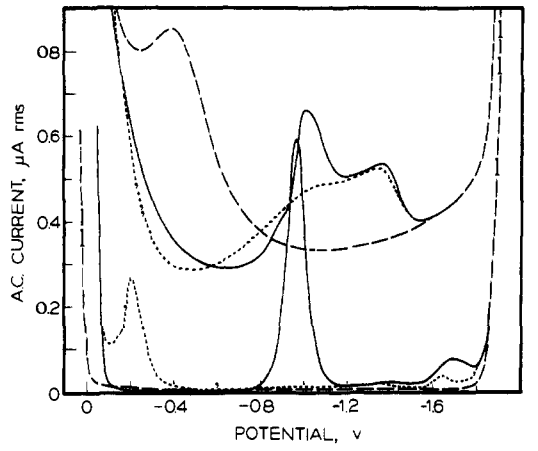

Figure 8. Ac polarograms of NAD^+ (1.20 mM) in pH 9.5 KCl/carbonate buffer. The three sets of curves correspond to the in-phase and quadrature current components for the supporting electrolyte alone (dashed line), NAD^+ solution before electrolysis (solid line), and NAD^+ solution after electrolysis at −1.2 V (dotted line).

Table IV. Sequential Electrolyses of a Solution of NAD^+ and Its Electrolytic Wave I Reduction Product[a]

Electrolysis potential	n value[b]	NAD^+ Enzymatic concn, mM	NAD^+ Polarographic current,[f] μA	Absorbance at 340 nm[g]	Reduction product current,[h] μA	Nicotinamide current,[i] μA
		1.10[c]	2.13	0.011	0.00	
−1.20[d]	1.02	0.01	0.00	0.785	1.76	0.27[j]
−0.10[e]	0.94	1.06	2.06	0.018	0.00	
−1.20[d]	0.96	0.01	0.00	0.759	1.70	0.34[j]

[a] Solution: 0.5 M carbonate buffer; pH 9.0. [b] Values of n are based on the initial NAD^+ concentration of 1.10 mM. [c] Original concentration of NAD^+, before electrolysis, as determined enzymatically. [d] Potential on the limiting portion of the first cathodic polarographic wave. [e] Potential on the limiting portion of the anodic wave. [f] Current for first cathodic wave. [g] Absorbance of an aliquot of the electrolysis solution after a one-fifth dilution with the electrolysis buffer. [h] Current for anodic wave produced in reduced solution. [i] Current for small cathodic wave observed in reduced solution. [j] Limiting currents correspond to nicotinamide concentrations of 0.051 and 0.064 mM.

grams of the electrolyzed solutions. Two new waves appeared: an anodic wave ($E_{1/2}$ = −0.25 V; oxidation of dimer to NAD^+) and a small cathodic wave ($E_{1/2}$ = −1.6 to −1.7 V; reduction of nicotinamide). In pH 9.5 buffer 5, the anodic wave is diffusion controlled and proportional to concentration; its I of 2.06 corresponds to a diffusion coefficient of 2.87×10^{-6} cm^2/sec (64% that of NAD^+). A maximum of the first kind appears at dimer concentration exceeding 0.2 mM. Near mercury discharge, the wave exhibits a sharp excursion toward zero current due to mercury oxidation and reaction with adenine to form a film on the electrode surface. $E_{1/2}$ is independent of h, but shifts from −0.37 to −0.27 V with increasing concentration; this increasing difficulty of oxidation is due to the surface activity of the adenine moiety, which inhibits the electron-transfer process; thus, $E_{1/2}$ of the NMN dimer is independent of concentration but becomes more positive on addition of adenine nucleotides to the solution. At 0.19 mM dimer, the wave slope ($E_{1/4} - E_{3/4}$) is 53 mV.

Ac polarography (Figure 8) shows the absence of both faradaic reduction peaks and the presence of dimer oxidation peak at −0.2 V; presence of the tensammetric peak at −1.35 V supports nonadsorption of dimer in the wave II potential region.

NAD^+ solutions have a single ultraviolet absorption maximum at 259 nm (ε 17,800; absorption by pyridine and adenine moieties).[9] The electrolyzed solutions had maxima at 259 (ε 32,000 ± 1,300) and 340 nm (ε 6890 ± 110); the wavelengths agree with those reported for the dimer.[17]

Enzymatic analysis showed that the NAD^+ concentration decreased on electrolysis to less than 1% of its original value; enzymatic analysis for NADH was negative.

On voltammetric examination at the mercury pool electrode, HMDE and PGE, when the scan toward more negative potential was begun at −0.5 V, no cathodic current due to NAD^+ was seen; on the reverse sweep, an anodic peak appeared at −0.16 V (no additional peaks appear on continuing the scan to 0.7 V at the PGE); on further sweep reversal, the −1.0 V NAD^+ peak appeared. Repetitive cycling over a potential range, which included the two peaks, produced patterns nearly identical with those seen for NAD^+. These results show that the 1e product produced on controlled potential electrolysis (a rather lengthy experiment) is the same as that produced on cyclic voltammetry (a rapid experiment). Most NAD radicals must react quickly to form a stable product. The greenish-yellow color cannot be due to an intermediate in the normal reduction; a small portion of radicals, however, may lead to a less stable intermediate.

The items listed in Table IV were measured before and after each of a series of electrolyses at a mercury pool electrode. After initial electrolysis at −1.2 V, NAD^+ had vanished; the solution absorbed strongly at 340 nm, and gave anodic and cathodic polarographic waves, as previously discussed. After the second electrolysis at −0.1 V, the NAD^+ concentration was nearly restored with corresponding loss in the 340-nm absorbance and anodic wave. During the three electrolyses, about 1% NAD is lost due to slow hydrolysis (increase in nicotinamide over that originally present as an impurity) and perhaps to a process associated with the greenish-yellow color.

After electrolysis of NAD^+ at −1.2 V, the nicotinamide wave was higher at pH 9.5 than at pH 9.0, which correlates with the more rapid NAD^+ decomposition at the higher pH. The current on further electrolyses at a potential on the nicotinamide wave plateau (−1.8 V; pH 9.6 buffer 6) rapidly decreased (15 min) to background level; the coulombs passed correspond to the nicotinamide determined polarographically; the increase in 340-nm absorbance corresponds to the expected amount of 1,6-dihydronicotinamide (ϵ_{340} 4200).[5] Enzymatic tests for 1,4-NADH were negative. Polarography of the final solution revealed no nicotinamide wave, an unchanged dimer anodic wave, and a new anodic wave ($E_{1/2}$ = −0.05 V) due to oxidation of the 2e nicotinamide reduction product.[5,6] This experiment shows that the cathodic wave seen in the NAD^+ wave I electrolyzed solutions is due to reduction not of dimer but of nicotinamide. When the potential was held at −1.8 V for an additional 4 hr after completion of nicotinamide reduction, 340-nm absorption remained constant and enzymatic tests for 1,4-NADH were again negative. Comparison of PGE voltammograms after electrolysis at −1.2 V and after 4 hr at −1.8 V showed no development of NADH. Overall, the data show that the dimer is not reduced within the available potential range to a dihydropyridine species (−1.8 V corresponds to the foot of solution discharge; cf. Figure 3). However, on electrolysis at more negative potential on rising solution discharge (e.g., −1.85 to −1.90 V), 340-nm absorption slowly increased; this phenomenon was not investigated further.

2. Wave II Process. Electrolyses of NAD^+ on the wave II plateau (−1.8 V) in pH 9.6 buffer 6, where the wave is

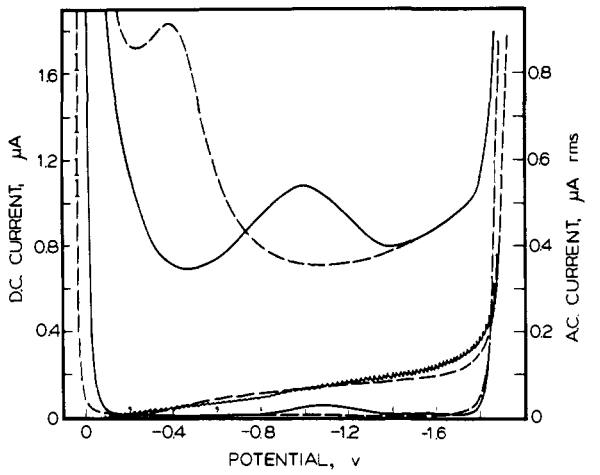

Figure 9. Dc and ac polarograms of NADH (1.20 m*M*) in pH 9.3 KCl/carbonate buffer. Ac polarograms: solid lines represent in-phase and quadrature current components for solutions; dashed lines represent corresponding background currents.

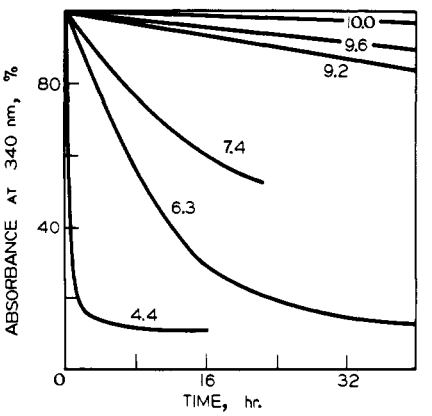

Figure 10. Effect of pH on stability of the NAD dimer. Buffer solutions and dimer concentration above pH 9: carbonate and 2.16×10^{-5} *M*; below pH 9, McIlvaine and 1.89×10^{-5} *M*. All solutions stored under air at room temperature.

well defined and diffusion controlled, gave an average *n* of 1.98 (eight electrolyses of 0.32-1.26 m*M* NAD^+; standard deviation = 0.11); the current decreased to background level. No transient color appeared; the electrolyzed solution was faint yellow.

Electrolyzed solutions had maxima at 250 and 341 nm. Enzymatic analysis showed a decrease in NAD^+ to less than 1% of its initial concentration and an average 54% conversion to 1,4-NADH. In order to demonstrate that 1,4-NADH was not chemically altered after being formed electrochemically, authentic 1,4-NADH was electrolyzed for 4 hr; no changes occurred in ultraviolet spectrum or enzymatic activity. In another experiment, electrolysis of NAD^+ at −1.8 V gave a 52% conversion to 1,4-NADH; continued electrolysis for 4 hr only increased the 1,4-NADH by 0.5%.

Polarograms of electrolyzed solutions revealed absence of the two NAD^+ cathodic waves and presence of an anodic dimer wave corresponding to an average of 11% NAD^+; the *n* of 1.98 is, accordingly, 5-6% high. The discrepancy is at least partially accounted for by the 2e electrolysis of nicotinamide (ca. 4 mol % present); nonenzymatically active α-NAD^+ may also be present.

On voltammetry at the PGE, no NAD^+ reduction was seen on scanning negatively from −0.6 V; after sweep reversal (−1.3 V), a small anodic peak appeared at −0.17 V (dimer oxidation) as well as a much larger peak at 0.42 V (dihydropyridine oxidation). On further sweep reversal (0.6 V), a cathodic peak appeared at −0.95 V (NAD^+ reduction). A final sweep reversal (−1.3 V) revealed an increased first anodic peak (dimer oxidation) and a decreased second one. Voltammetry, therefore, involved oxidation of both 1e and 2e reduction products to NAD^+, which was subsequently reduced to the 1e product.

The ac polarographic behavior of the 2e reduction product in buffer 5 is similar to that of authentic 1,4-NADH (Figure 9), which does not exhibit faradaic peaks but does show adsorption behavior. At potential prior to and near the ecm, the dl capacity is suppressed (also seen on dc polarography); at more negative potential, NADH is desorbed, producing a broad tensammetric hump centering at −1.0 V. Beyond −1.45 V (region of wave II process), the capacity is the same as for background alone.

Chemical Properties of Dimer and Dihydropyridine Species. The effects of oxygen and pH on the dimer were studied on NAD^+ solutions electrolyzed at −1.2 V at pH 6.4, 7.2, 8.0, and 9.8 (McIlvaine or carbonate buffer). Three aliquots were taken from each solution; two were stored under N_2 or O_2 at room temperature; the third was immediately analyzed polarographically, spectrophotometrically, and enzymatically; after 24 hr, the stored aliquots were similarly examined. The effect of O_2 relative to N_2 is marginal. Above pH 9, O_2 did not accelerate decomposition; below pH 9, only a small effect was observed. In no instance was H_2O_2 detected polarographically.

With decreasing pH, both products decompose at an increasing rate (Figure 10); at any pH, the dimer is less stable than the dihydropyridine. During hydrolysis, the 340-nm band of NAD^+ wave I and wave II electrolyzed solutions decreases and a more intense band develops at 280 nm; the 260-nm band due primarily to adenine changes very little.

In carbonate buffers above pH 9, the dimer is relatively stable; in McIlvaine buffers below pH 8, it rapidly decomposes (Figure 10; the leveling off of 340-nm absorption is due to the foot of the 280-nm band extending past 340 nm). At pH 6.3, the dimer had a half-life of 8 hr; during decomposition, an isosbestic point formed at 315 nm. The final 280-nm band had an ϵ of 18,000 after accounting for adenine absorption. The decrease in anodic dimer wave with time (pH 6-8) correlates with loss in 340-nm absorption.

At pH 4.3, the dimer half-life is 16 min; that of 1,4-NADH is 30 min. After correction for 280-nm band tail absorption, the 340-nm absorption and dimer anodic current again decreased at the same rate. At pH 2.2, the 280-nm band instantly formed but then rapidly decreased in intensity; evidently, the dimer forms an acid-catalyzed decomposition product, which absorbs at 280 nm and decomposes to a secondary product, which does not absorb at 280 nm.

The slow decrease in dimer concentration above pH 9 is due to oxidation to NAD^+, which, as noted, is independent of the presence of oxygen. The 340-nm band decreases without concomitant formation of the 280-nm band; the anodic wave also decreases; the NAD^+ cathodic wave appears but never reaches its expected height, since NAD^+ slowly hydrolyzes above pH 9.

Nature of the Electrode Processes

Redox Path. The reaction scheme outlined in Figure 11 best fits the available data (spectrophotometric, chemical, enzymatic, electrochemical) from past studies, as well as the present study, of NAD^+, $NADP^+$, and $DNAD^+$. Reversible 1e addition to the pyridinium ion (I) to produce a free radical (II) (source of wave Ic) is followed by irreversible dimerization to III, which is largely the 4,4′ with some of the 6,6′ and 4,6′ forms, reflecting the transition from the

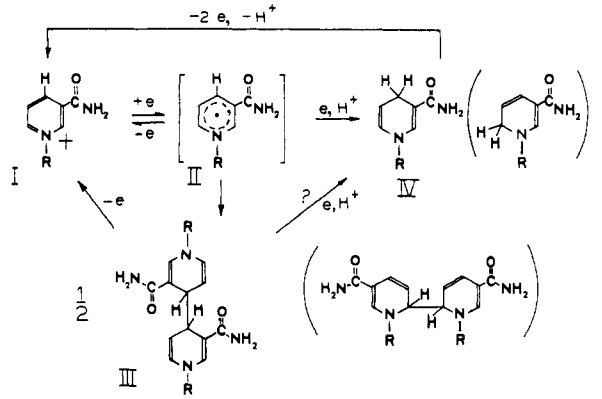

Figure 11. Reaction paths for the electrochemical behavior of nicotinamide adenine dinucleotide, related compounds, and their corresponding reduction products.

6,6′ isomer in the case of nicotinamide itself[5] to the 4,4′ form as the substituent on the pyridine nitrogen increases in size.[6] At considerably more negative potential, the pyridinium ion is reduced to a dihydropyridine (IV) via 1e reduction of the free radical (source of wave IIc). The wave II product is largely 1,4-NADH but some 1,6-NADH is also formed. At sufficiently positive potential, both dimer and dihydropyridine are oxidized to the original nucleotide. The dimer is not directly reduced electrochemically within the available potential range (cf. subsequent discussion).

Since the free radical dimerizes with a rate constant of about $10^6\ M^{-1}\ \text{sec}^{-1}$ (cf. below), dimerization would be essentially complete under DME polarographic conditions. The appearance of wave II at a potential where the dimer is stable to reduction indicates that the second electron transfer is very rapid compared with dimerization or that dimerization occurs away from the interface in the diffusion layer; the data, cyclic voltammetric patterns in particular, support the second electron transfer being more rapid.

The basis for postulating involvement of a proton in the overall electrode process is NADH formation. The sequence of addition of electrons and protons could be (a) e, e, H^+ or (b) e, H^+, e. If protonation of the neutral free radical is very rapid compared with its dimerization, either sequence could be competitive over the dimerization reaction in producing the dihydropyridine; otherwise, sequence (a) would be more likely. The behavior in nonaqueous media[18] favors concerted electron-proton addition.

Product Composition and Structure. Ultraviolet spectral characterization of electrolytically prepared 1-substituted 3-carbamoyldihydropyridines has been discussed.[5,6] Above 240 nm, most 1-substituted 3-carbamoylpyridinium ions show a single absorption band at about 410 nm for 1,2-dihydropyridines and 350 nm for 1,4-dihydropyridines, and two bands at about 265 and 360 for 1,6-dihydropyridines.[19]

The molar absorptivities at 260 and 340 nm of the NAD-derived dimer prepared in the present investigation are close to those of an isolated electrochemically prepared dimer[17] and similar to those of a dimer (not isolated) prepared by pulse radiolysis.[20] The dimer 260-nm absorption is greater than that expected from its two adenine moieties, implying absorption at two wavelengths by the nicotinamide moiety and, in turn, at least some dimerization at the 6 position. Nevertheless, workers,[17] who isolated the product, regarded the 4,4′ structure as more likely, based in part on NMR spectra.

The 4,4′ structure is more acceptable than the 6,6′ with respect to steric interactions between the bulky N substituents on the reduced nicotinamide rings; however, the 3-carbamoyl group also protrudes from the reduced pyridine ring and its steric effect must be considered. Molecular models of the *dl* form of the 4,4′ dimer suggest that at least one amide function must be twisted out of the plane of the adjacent vinyl group in order to achieve dimerization; for the meso form, both amide groups must be twisted. For the 6,6′ dimer, however, very little amide group deformation is necessary, although moderate interaction between N substituents is seen. Amide deformation may be sufficient to hinder to some extent 4,4′ dimer formation.

The NMN dimer, which also has bulky N substituents, appears to have largely a 6,6′ or 4,6′ structure based on its spectrum,[6] which, unlike that of the NAD dimer, is due only to the nicotinamide moiety.

Based on all available evidence, electrolysis on the NAD^+ wave I plateau produces a mixture of isomers. Although formation of a 2,2′ dimer is unlikely, based on steric interactions evident from molecular models, the transient greenish-yellow color seen during electrolysis may be due to formation of a small amount of such an isomer. Behavior analogous to that of the corresponding dihydropyridine might be expected; 1,2-NADH has an absorption maximum at 395 nm and is much less stable in slightly alkaline solution than 1,4- or 1,6-NADH;[21] the yellow color is lost on hydrolysis. The results of controlled potential coulometry and reversal coulometry[22] at pH 9–10 and systematic analysis of the resulting solutions prove that most NAD^+ is directly converted to relatively stable dimeric species which do not absorb appreciably in the visible.

Similarly, NAD^+ wave II electrolyzed solutions likely contain a mixture of 1,4- and 1,6-dihydro isomers plus a small percentage of dimer. Typically, analysis shows 54% enzymatically active 1,4-NADH and 11% dimer. Analysis of the spectral data[7] using literature molar absorptivities for the various species involved,[9,19,21] and of the faradaic *n* values, is in accord with the remaining 35% product being 1,6-NADH.

The acid-catalyzed hydrolysis of the reduction products involving the 4,5-C=C bond of a 1,6-dihydropyridine is an example of enamine nucleophilicity[23] and accounts for loss of 340-nm absorption and concomitant increase in 280-nm absorption, which is due to the

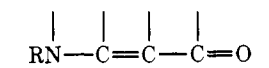

chromophore.[24] Hydrolysis of the 5,6 double bond of a 1,4 reduced pyridine would probably produce the same chromophore;[21a,23a] however, hydrolysis of a 1,2 reduced pyridine produces no new increase in absorption.[21a]

Although it would perhaps have been useful to have isolated the dimeric and dihydropyridine products and to have determined their exact composition and structure, it seemed questionable as to whether such a detailed study would yield information whose amount and importance would be commensurate with the effort required; e.g., a chromatographic study to determine the homogeneity of the products would not be expected to yield definitive results due to their moderate instability.

Charge-Transfer Reversibility. The first electron transfer to NAD^+ has been claimed to be reversible based on a log i–E plot[25] and cyclic voltammetric curves;[26b] however, substantial proof has not been offered. Radical formation has been indicated by cyclic voltammetry[26a] and chronopotentiometry;[27] the published patterns, however, show only a small oxidation peak or inflection.

In the present investigation, the slope of NAD^+ wave I was generally greater than that for a reversible 1e transfer. $E_{1/2}$ became more positive with increase in concentration or

Table V. Second-Order Dimerization Rate Constants for Free Radicals from NAD^+ and Related Compounds

Compd	pH[b]	Scan rate, V/sec	Rate constant[a] at 30° k_d, M^{-1} sec^{-1}	n	s, M^{-1} sec^{-1}	E_a,[c] kcal mol^{-1}
NAD^+	5.0	15–38	2.2×10^6	11	0.6	9
	9.0	13–26	2.4×10^6	3	2.1	
$NADP^+$	5.0	20–60	4.3×10^6	3	0.8	9
	9.0	20–60	1.6×10^6	3	2.6	
$DNAD^+$	9.0	20–36	1.7×10^6	3	2.3	

[a] Mean value of k_d is given together with standard deviation, s, for n measurements. [b] Buffer 3 was used at pH 5 and buffer 4 at pH 9. [c] Activation energies are based on Arrhenius plot of log k_d vs. T^{-1}, between 7 and 50°.

drop time; for a reversible electrode process in the absence of adsorption, such shifts are indicative of irreversible dimerization subsequent to charge transfer.[28] The latter is supported by the difference in the cyclic voltammetric patterns at slow and rapid scan rates, and the increase in the i_{pa}/i_{pc} ratio with increasing v (Figure 7). The 60-mV separation of peak potentials supports the reversible 1e nature of the redox couple. $NADP^+$ and $DNAD^+$ behave similarly.

Dimerization Rate Constants. The dimerization rate constant, k_d, of the NAD free radical, based on a chronopotentiometrically estimated free radical half-life of less than 1 msec,[27] should exceed 10^6 M^{-1} sec^{-1}; a k_d of 6.9×10^7 M^{-1} sec^{-1} has been determined by pulse radiolysis.[20]

Three approaches[16,29] for calculating k_d from cyclic voltammetric data are pertinent; their application to nicotinamide and coenzyme model compound radicals has been described.[5,6] Rate constants for the free radicals derived from NAD^+, $NADP^+$, and $DNAD^+$, calculated using Nicholson's peak current method,[16] are given in Table V; application of Saveant's approach[29] gives k_d values 10 to 15% higher.

The low activation energies of 9 kcal/mol support the rapid nature of the reaction and are in general agreement with dimerization processes for neutral free radicals where electronic repulsions are not involved. The corresponding calculated frequency factors of 7×10^{12} M^{-1} sec^{-1} for NAD and 1×10^{13} for NADP are within the range expected for reaction between neutral free radicals, where no extensive solvation difference exists between reactant and product.

The difference of an order of magnitude in k_d for NAD free radical dimerization determined by pulse radiolysis and by polarography is disturbing, especially since k_d values for the 1-methylnicotinamide (MCP^+) free radical determined by the two approaches agree quite well.[6] Since the polarographic measurement is related to phenomena at an interface, adsorption and diffusion may affect the rate measurement. Due to presence of the adenine moiety, NAD^+ and its reduction products are strongly adsorbed. While MCP^+ is only slightly adsorbed, its dimeric and dihydropyridine reduction products are strongly and moderately adsorbed, respectively, due to their hydrophobic alkyl substituent. The relative values of k_d for NAD and MCP free radicals found in the present studies (2×10^6 and 6×10^7) are supported by the statement in another polarographic study[30] that NAD and NADP radicals have an appreciably longer lifetime than those of the *N*-alkyl models.

Since the k_d values for $NADP^+$ and $DNAD^+$, which are also adsorbed, are comparable with k_d for NAD^+, they may also be low compared with those which would be determined by pulse radiolysis. It is also possible that k_d for NAD, determined by pulse radiolysis, is too high.

Oxidation and Reduction of the Dimers. The pH independence of dimer oxidation above pH 6 is consistent with the redox scheme of Figure 11. Below pH 6, the potential becomes more positive with decreasing pH, indicating proton loss during oxidation, which may result from protonation of the dimer at lower pH; this is consistent with promotion of catalytic hydrogen evolution at the DME by the dimer and its acid-catalyzed hydrolysis.

The ease of dimer oxidation is remarkable. Electrochemical oxidation or reduction of carbon-carbon single bonds is generally limited to systems where one or both carbons have an oxygen bond,[31a] e.g., semiquinone type dimers as alloxantin.[31b] At pH 9.6, the NAD dimer is oxidized at the PGE at about 0.6 V less positive than NADH. Simple inductive effects cannot account for the magnitude of the enhancement. An important factor may be weakening of the connecting bond due to molecular crowding caused by interaction between substituents on the pyridine ring.

A small cathodic wave close to background discharge in a solution of the NAD^+ wave I electrolysis product has been attributed[25b] to direct reduction of dimer to 1,4-NADH, since 1,4-NADH activity slowly developed on further electrolysis at −1.84 V; the slow rate was ascribed to mercury surface adsorption phenomena. However, the cathodic wave was not examined. The NADP dimer gave virtually identical results.[32] In the present study, a similar cathodic wave, seen in solutions of NAD^+ and NMN^+ wave I electrolysis products, has been shown to be due to free nicotinamide, present as an impurity and formed by decomposition of NMN^+ and NAD^+ during electrolysis under slightly alkaline conditions.[5,6,33] Capacitance data indicate an absence of adsorption phenomena in the wave II potential region. The NAD dimer was not reduced on electrolysis as negative as −1.8 V; however, when the potential was shifted into the background discharge region (−1.85 to −1.90 V; cf. Figure 3), the 340-nm absorption slowly increased, suggesting conversion of dimer to more highly absorbing dihydropyridine. Nearly identical behavior was found for NMN^+.[6]

In view of the absence of adsorption, the slow formation of dihydropyridine species from dimer suggests that a direct reduction is not involved (dc wave is absent), unless, coincidentally, the rising portion of the dimer reduction wave occurs just beyond solution discharge; this seems unlikely, however, since the potential of solution discharge of final wave I electrolyzed solutions is identical with that for the background electrolyte alone. Indirect reduction may result via interaction of reduction products of background discharge with dimer, e.g., hydrogen radicals. Further investigation of this point is necessary.

Adsorption Phenomena. The steps or waves that appear on dc polarography of NAD^+ in addition to the two 1e reduction steps can be explained, largely on the basis of ac polarography, in terms of adsorption phenomena, e.g., adsorption of NAD^+ at the interface, replacing solvent molecules and background electrolyte ions. Thus, the polarographic patterns of NAD^+ in buffers 5 and 6 represent two extreme cases (Figure 4). Those in Et_4NCl solutions are less complicated due to desorption of NAD^+ prior to the first reduction step; as the concentration of Et_4NCl is decreased and that of KCl is increased, the desorption process shifts to more negative potential.

In KCl/carbonate buffer, the capacity current is depressed due first to NAD^+ adsorption and then to dimer adsorption up to a potential intermediate between waves 1 and 11 (ca. −1.3 V) where the dimer is desorbed; as the potential becomes more negative, the background electrolyte cation (K^+) displaces the dimer because of increasing coulombic attraction of K^+ to the electrode. The dimer is more strongly adsorbed if its surface activity is increased (by increasing ionic strength, lowering temperature, or increasing its interfacial concentration). During desorption, alteration

of the mercury surface tension promotes solution stirring, thereby enhancing the wave I limiting current; the capacity wave thus behaves similarly to maxima of the second kind,[34] in being proportional to mercury height, ionic strength, and NAD^+ concentration, and in being suppressed by surfactants such as Triton and Et_4N^+.

In Et_4NCl/carbonate buffer, the capacity current is essentially identical with that for the background electrolyte alone after the capacity wave or ac tensammetric peak at approximately −0.6 V. Before the capacity step, NAD^+ is adsorbed; after the step, Et_4N^+ is preferentially adsorbed.

Comparison of the behavior of NAD^+ with, for example, that of NMN^+, indicates that the adenine moiety plays a major role in the adsorption process; NAD^+ behaves similarly to nearly all adenine nucleosides and nucleotides[35] in being strongly adsorbed in the potential region prior to and in the vicinity of the ecm, and in giving rise to desorption peaks at more negative potential. Similarly, the adenine or purine-related moiety of $NADP^+$, $DNAD^+$, $DNADP^+$, and α-NAD^+ causes adsorption behavior characteristic for each compound. On addition of Et_4NCl, adsorption of the dinucleotides beyond the ecm is minimized due to preferential adsorption of Et_4N^+; the dc polarographic patterns of the dinucleotides are then very similar to each other and to NMN^+.

Acknowledgment. The authors thank the National Science Foundation and the Horace H. Rackham School of Graduate Studies of the University of Michigan, which helped support the work described.

References and Notes

(1) Address correspondence to this author.
(2) NADH is taken to mean 1,4-NADH; in the case of other isomers arising from the reduction of NAD^+, the reduction site is specified.
(3) H. F. Fisher, E. E. Conn, B. Vennesland, and F. H. Westheimer, *J. Biol. Chem.*, **202**, 687 (1953); M. E. Pullman, A. San Pietro, and S. P. Colowick, *ibid.*, **206**, 129 (1954).
(4) B. Janik and P. J. Elving, *Chem. Rev.*, **68**, 295 (1968); A. L. Underwood and J. N. Burnett, "Electroanalytical Chemistry", Vol. 6, A. J. Bard, Ed., Marcel Dekker, New York, N.Y., 1972, pp 1–85; P. J. Elving, J. E. O'Reilly, and C. O. Schmakel, "Methods of Biochemical Analysis", Vol. 21, D. Glick, Ed., Wiley-Interscience, New York, N.Y., 1973, pp 287–465.
(5) C. O. Schmakel, K. S. V. Santhanam, and P. J. Elving, *J. Electrochem. Soc.*, **121**, 345 (1974).
(6) C. O. Schmakel, K. S. V. Santhanam, and P. J. Elving, *J. Electrochem. Soc.*, **121**, 1033 (1974).
(7) C. O. Schmakel, Ph.D. Dissertation, The University of Michigan, 1971.
(8) S. P. Colowick and N. O. Kaplan, "Methods in Enzymology", Vol. III, Academic Press, New York, N.Y., 1957, p 890.
(9) The ultraviolet spectrum of NAD^+ exhibits a single band at 259 nm (ϵ 17,800)[10] due to absorption by both the adenine and pyridine moieties; with the formation of NADH, absorption due to the pyridine moiety shifts to a longer wavelength so that two bands are seen, one at 259 nm (ϵ 14,400)[10b] and the other at 338 nm (ϵ 6220).[10]
(10) (a) A. D. Winer, *J. Biol. Chem.*, **239**, PC3598 (1964); (b) J. M. Siegel, G. A. Montgomery, and R. M. Bock, *Arch. Biochem. Biophys.*, **82**, 288 (1959).
(11) A catalytic hydrogen reduction occurs when a compound is present whose protonated adduct is more easily reducible, e.g., has a lower activation energy in respect to net addition of an electron to the proton, than the uncomplexed proton itself.
(12) Except where otherwise specified, an alternating voltage of 50 Hz and 5-mV peak amplitude (3.5 mV root mean square) was employed at a controlled 3-sec drop time with recording of the instantaneous ac current at the end of the drop life. In the frequency variation studies, a 10-mV peak amplitude and a natural drop time were used.
(13) Both the in-phase and quadrature components of the total alternating current are shown in Figure 2 along with the corresponding curves for the supporting electrolyte alone. In a potential region where a faradaic step does not occur, the quadrature (out-of-phase) current component is proportional to the differential double layer capacity at the solution–electrode interface and thus provides a convenient index to adsorption at the interface of an electroactive species and its products.
(14) D. E. Smith and T. G. McCord, *Anal. Chem.*, **40**, 474 (1968).
(15) Peak IIc may also be due in part to reduction of nicotinamide which is present as a minor impurity (cf. discussion of controlled potential electrolysis).
(16) R. S. Nicholson, *Anal. Chem.*, **37**, 667 (1965).
(17) R. W. Burnett and A. L. Underwood, *Biochemistry*, **7**, 3328 (1968).
(18) K. S. V. Santhanam and P. J. Elving, *J. Am. Chem. Soc.*, **95**, 5482 (1973).
(19) G. Maggiora, H. Johansen, and L. L. Ingraham, *Arch. Biochem. Biophys.*, **131**, 352 (1969); K. Wallenfels, *Ciba Found. Study Group*, **2**, 10 (1959); K. Wallenfals and M. Gellrich, *Chem. Ber.*, **92**, 1406 (1959).
(20) E. J. Land and A. J. Swallow, *Biochim. Biophys. Acta*, **162**, 327 (1968).
(21) (a) S. Chaykin, L. King, and J. G. Watson, *Biochim. Biophys. Acta*, **124**, 13 (1966); (b) S. Chaykin and L. Meissner, *Biochem. Biophys. Res. Commun.*, **14**, 233 (1964).
(22) A. J. Bard and K. S. V. Santhanam, "Electroanalytical Chemistry", Vol. 4, A. J. Bard, Ed., Marcel Dekker, New York, N.Y., 1970, pp 215–315.
(23) (a) E. M. Kosower, "Molecular Biochemistry", McGraw-Hill, New York, N.Y., 1962, p 166; (b) D. J. McClemens, A. K. Garrison, and A. L. Underwood, *J. Org. Chem.*, **34**, 1867 (1969).
(24) R. M. Burton and N. O. Kaplan, *Arch. Biochem. Biophys.*, **101**, 150 (1963).
(25) (a) J. N. Burnett, Ph.D. Dissertation, Emory University, 1965; (b) J. N. Burnett and A. L. Underwood, *Biochemistry*, **4**, 2060 (1965).
(26) (a) A. J. Cunningham, Ph.D. Thesis, Emory University, 1966; (b) A. J. Cunningham and A. L. Underwood, *Biochemistry*, **6**, 266 (1967).
(27) A. M. Wilson and D. G. Epple, *Biochemistry*, **5**, 3170 (1966).
(28) (a) S. G. Malranovskii, *Dokl. Akad. Nauk SSSR*, **110**, 593 (1956); (b) J. Heyrovsky and J. Kuta, "Principles of Polarography", Academic Press, New York, N.Y., 1966, p 396; (c) R. Bonnaterre and G. Cauquis, *J. Electroanal. Chem.*, **32**, 199 (1971).
(29) J. M. Saveant, *Electrochim. Acta*, **12**, 999 (1967).
(30) H. Berg, private communication; H. Hanschmann, Doctoral Dissertation, Friedrich Schiller University, Jena, DDR, 1970.
(31) (a) L. Horner and H. Lund, "Organic Electrochemistry", M. M. Baizer, Ed., Marcel Dekker, New York, N.Y., 1973, pp 763–766; (b) W. A. Struck and P. J. Elving, *J. Am. Chem. Soc.*, **86**, 1229 (1964).
(32) A. J. Cunningham and A. L. Underwood, *Arch. Biochem. Biophys.*, **117**, 88 (1966).
(33) As expected, the wave is not observed in electrolyzed solutions of 1-methylnicotinamide;[6] the latter compound decomposes under alkaline conditions via hydrolysis of the amide function.
(34) J. Heyrovsky and J. Kuta, "Principles of Polarography, Academic Press, New York, N.Y., 1966, p 452; L. Meites, "Polarographic Techniques", Wiley, New York, N.Y., 1965, p 305.
(35) B. Janik and P. J. Elving, *J. Am. Chem. Soc.*, **92**, 235 (1970).